2024 IEEE International Conference on Robotics and Automation (ICRA 2024)
May 13-17, 2024. Yokohama, Japan

Coordinated Landing Control for Cross-Domain UAV-USV Fleets Using Heterogeneous-Feature Matching

Jianing Ding, Hai-Tao Zhang*, Bin-Bin Hu

Abstract— **Coordinated landing control for multiple unmanned aerial vehicles (UAVs) on appropriate multiple unmanned surface vehicles (USVs) is an urgent yet challenging mission with the tremendous development of modern marine industry. To this end, we propose a coordinated multiple UAV-USV landing control algorithm via heterogeneous-feature matching. Specifically, the heterogeneous landing features of different UAVs and USVs are extracted to establish a dynamic UAV-USV cooperative landing ability mapping for the cross-domain UAV-USV fleets (CDUUFs). Then, by incorporating suitable allocation with UAV-USV landing convergence and collision avoidance among UAVs into constraints with the assistance of both control Lyapunov functions (CLFs) and control barrier functions (CBFs), the multiple UAV-USV landing control problem is formulated as a constraint-based optimization one. Therein, slack variables are introduced to fulfill the assignment and facilitate the searching of a balanced solution between control performance and landing safety. Finally, extensive simulations are conducted to substantiate the effectiveness of the present multiple UAV-USV landing control law.**

I. Introduction

In recent years, cross-domain UAV-USV fleets (CDUUFs, including unmanned aerial vehicles and unmanned surface vehicles) have been demonstrated to play a pivotal role in various engineering applications, such as environmental exploration and monitoring [1], collective search [2], and target convoying [3], [4] due to their low cost, superior efficiency, flexibility, security and robustness [5]–[7].

Initially, most of the works only focus on the coordinated control of single-domain unmanned systems. For instance, several UAVs collaboratively transporting a payload with environmental obstacles was investigated in [8]. A minimum control (MINCO) trajectory representation was developed in [9] for UAVs to conduct spatial and temporal trajectory deformation. However, due to the limitations imposed by UAVs, such as low payload capacity and battery endurance time, they may become vulnerable to environmental perturbations, thereby elevating the likelihood of incidents and losses. Additionally, research efforts have been devoted to the coordination of USVs [10], characterized by larger effective payload capacity and expanded accommodation space. In this pursuit, a guiding-vector-field algorithm was proposed in [11] to form a *spontaneous-ordering* platoon and execute the path navigation for USVs. Nevertheless, USVs are naturally limited to operating on 2D water surfaces, which hinders their ability to perceive the ever-changing surroundings and restricts their access to shallow shoals and narrow areas.

In order to address the limitations associated with coordinating UAVs or USVs individually within their respective domains, it becomes crucial to integrate UAVs with USVs and harness their collective strengths [12]. This rationale forms the basis for a typical application scenario involving coordinated landing missions of UAVs and USVs [13]. Precisely, when the UAV has completed its assigned mission or its residual battery energy descends below a predefined threshold, it can discern an appropriate USV among multiple USVs to land, then be retrieved or recharged to conduct a task again. Meanwhile, UAVs, acting as the eyes for USVs, can augment the environmental comprehension and decision-making process for USVs by expanding their perception range from 2D to 3D. For instance, a sliding-mode control scheme was proposed in [14] for the UAV-USV tracking and landing. A multi-layer nested 2D marker was used in [15], and then a learning-based detection, localization, and control framework was developed to land a UAV on a moving USV. Later, a model predictive control (MPC) approach was designed in [16] to handle harsh environmental conditions during the landing procedure. However, due to the intricate and arduous nature of multiple cross-domain UAV-USV cooperation, the aforementioned studies only concentrate on single-UAV single-USV situations. As for several preliminary attempts in this challenging multiple UAV-USV landing scenario, a manipulator-based assistance system on the USV was proposed in [17], which conserves landing space and enables the transport of multiple UAVs. A distributed landing auction algorithm was developed in [18] to minimize the energy consumption difference of the UAV group. However, the issue of multiple UAVs simultaneously landing on multiple USVs still remains an open problem. It is worth mentioning that the energy consumption model employed in [18] requires a rigorous assumption on the motion of the UAV, and the allocation is implemented only once, which limits its further application as well. Besides, existing multi-robot coordination works [19]–[21] typically

This work was supported in part by the National Key Research and Development Program of China under Grant 2022ZD0119601, in part by the National Natural Science Foundation of China under Grants 62225306, U2141235, and 61803168, and in part by the Guangdong Basic and Applied Research Foundation under Grant 2022B1515120069. (*Corresponding author: Hai-Tao Zhang*)

Jianing Ding and Hai-Tao Zhang are with the School of Artificial Intelligence and Automation, the MOE Engineering Research Center of Autonomous Intelligent Unmanned Systems, the Guangdong Engineering Technology Research Center of Fully Autonomous Unmanned Surface Vehicles, and the State Key Laboratory of Digital Manufacturing Equipment and Technology, Huazhong University of Science and Technology, Wuhan 430074, China, {djn@, zht@mail.}hust.edu.cn

Bin-Bin Hu is with the School of Mechanical and Aerospace Engineering, Nanyang Technological University, Singapore 637460, binbin.hu@ntu.edu.sg

separate task allocation from control implementation, leading to increased system design complexity and communication delays that may cause performance degradation.

Recently, a constraint-based task-execution algorithm was proposed in [22]–[24], where different task allocations and executions are interpreted through prioritization and control barrier functions (CBFs), respectively, and then are encoded as constraints in the minimum energy consumption optimization problem. This formulation naturally satisfies the long-term autonomy and provides a model accounting for the robot heterogeneity. Motivated by these works [22]–[24], we propose a unified multiple UAV-USV coordinated landing control algorithm via heterogeneous-feature matching. Specifically, the heterogeneous landing features of different UAVs and USVs are extracted to establish a matching mechanism for the calculation of the CDUUF cooperative landing ability. Then, by encoding allocation requirements, UAV-USV landing convergence, and collision avoidance among UAVs into constraints, the proposed landing controller is formulated to be a constraint-based optimization one, which thus can assign each UAV to the most suitable USV and generate control inputs for the UAVs. The contribution of this paper is two-fold.

1) Extract heterogeneous landing-related features from UAVs and USVs to facilitate appropriate UAV-USV matching.
2) Design an optimal coordinated landing controller for multiple UAVs on suitable USVs, which minimizes both energy cost and cooperative landing ability violations.

II. Problem Formulation

A. Preliminaries

To achieve a trade-off between control performance and landing safety of the CDUUFs, we first introduce some necessary definitions.

Definition 1. *(Control Lyapunov functions (CLFs)) [25] For a continuously differentiable function $V(x):\mathbb{R}^n\to\mathbb{R}^+$ and a typical affine control system*

$$\dot{x}=f(x)+g(x)u, \tag{1}$$

with the state $x\in\mathbb{R}^n$, input $u\in U\subset\mathbb{R}^m$, the locally Lipschitz continuous functions $f:\mathbb{R}^n\to\mathbb{R}^n$ and $g:\mathbb{R}^n\to\mathbb{R}^{n\times m}$, then $V(x)$ becomes a CLF for Eq. (1) *if there exist continuous and positive definite functions $W_1(x)\in\mathbb{R}^+, W_2(x)\in\mathbb{R}^+, W_3(x)\in\mathbb{R}^+$ and $u\in U$ such that the following inequalities hold for all $x\in\mathbb{R}^n$,*

$$\begin{aligned}&W_1(x)\le V(x)\le W_2(x),\\&L_fV(x)+L_gV(x)u+W_3(x)\le 0,\end{aligned} \tag{2}$$

where L_f and L_g denote the Lie derivatives of $V(x)$ in the directions f and g, respectively.

In Definition 1, the CLF $V(x)$ accounting for the control performance of a vehicle will finally converge to zero under the condition (2), i.e., $\lim_{t\to\infty}V(t)=0$.

Definition 2. *(Control barrier functions (CBFs)) [26] Let $C\subset\mathbb{R}^n$ be the safe set of a continuously differentiable function $h:\mathbb{R}^n\to\mathbb{R}$, i.e. $C=\{x\in\mathbb{R}^n:h(x)\ge 0\}$, then h becomes a CBF if there exists an extended class K_∞ function γ such that for Eq.* (1) *the following inequality holds for all $x\in\mathbb{R}^n$,*

$$\sup_{u\in U}\{L_fh(x)+L_gh(x)u+\gamma(h(x))\}\ge 0. \tag{3}$$

Definition 2 illustrates that the state x can stay in the safe set C all along under the condition Eq. (3) due to the forward invariance property [26], i.e., $x(0)\in C\Rightarrow x(t)\in C,\forall t>0$.

Definition 3. *(Constraint-based optimization) For the CLF $V(x)$ and CBF $h(x)$ given in Eqs.* (2) *and* (3)*, respectively, a vehicle governed by the dynamics in Eq.* (1) *can be guaranteed asymptotic stability and safety simultaneously if the following quadratic programming optimization is addressed, i.e.,*

$$\begin{aligned}\min_{u,\delta}\quad&\frac{1}{2}u^{\intercal}H(x)u+p\delta^2\\ s.t.\quad&L_fV(x)+L_gV(x)u+W_3(x)-\delta\le 0\\&L_fh(x)+L_gh(x)u+\gamma(h(x))\ge 0,\end{aligned} \tag{4}$$

where $H\in\mathbb{R}^{m\times m}$ is a positive definite matrix, $p>0$ is a penalty constant, and δ is a slack variable used to ensure the solvability, which implies that the control performance can be sacrificed to always maintain the system's safety.

B. Cross-Domain UAV-USV Fleets

We consider a CDUUF composed of n_a UAVs represented by $\mathcal{V}_1=\{1,2,\dots,n_a\}$ and n_s USVs represented by $\mathcal{V}_2=\{1,2,\dots,n_s\}$, respectively.

The dynamics of each UAV is simplified to be a second-order integrator [27]

$$\begin{aligned}\dot{q}_i(t)&=p_i(t),\\\dot{p}_i(t)&=u_i(t),\end{aligned} \tag{5}$$

where $q_i(t)\in\mathbb{R}^3$, $p_i(t)\in\mathbb{R}^3$, and $u_i(t)\in\mathbb{R}^3$ are the position, velocity, and acceleration input of the i-th UAV, respectively.

The dynamics of each USV is assumed to be described by a second-order dynamic [28]

$$\begin{aligned}\dot{\eta}_j(t)&=\nu_j(t),\\\dot{\nu}_j(t)&=\tau_j(t),\end{aligned} \tag{6}$$

where $\eta_j(t)\in\mathbb{R}^3$, $\nu_j(t)\in\mathbb{R}^3$ and $\tau_j(t)\in\mathbb{R}^3$ are the position, velocity and control input of the j-th USV, respectively. Note that Eq. (6) implicitly contains $\eta_{j,z}(t)=0$, such dynamics is commonly utilized in previous works [29], and can be easily achieved by a hierarchical control framework.

In a practical coordinated landing task, the heterogeneous property of the CDUUF originates from their different features. For instance, the UAVs may have different body sizes and battery capacities. At the same time, the USVs are equipped with different-sized landing platforms and remaining charging energies, which thus pose challenging issues to

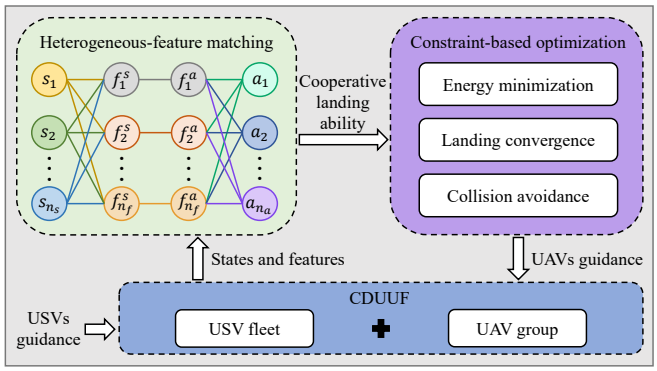

Fig. 1. System architecture. The USV fleet is guided externally, and the UAV group is controlled through the optimization framework.

match among these features and govern multiple UAVs to land on suitable USVs.

C. Problem Formulation

Problem 1. *(Multiple UAV-USV landing control) For a UAV group $\mathcal{V}_1$ governed by Eq.* (5) *and a USV fleet $\mathcal{V}_2$ governed by Eq.* (6)*, we design a constraint-based optimization framework to generate optimal control inputs $u_i, i \in \mathcal{V}_1$ for UAV i, such that*

$$\begin{aligned} &\lim_{t\to\infty} \alpha_{j,i}(t)\|q_i(t) - \eta_j(t)\| = 0, \quad \forall i \in \mathcal{V}_1, \\ &\|q_i(t) - q_k(t)\| \geq D_{\min}, \quad \forall t \geq 0, \forall i,k \in \mathcal{V}_1, i \neq k, \end{aligned} \tag{7}$$

with $\alpha_{j,i} \in \{0,1\}$ being the matching priority for USV j to UAV i, and $D_{\min} \in \mathbb{R}^+$ being the safe distance.

III. Main Results

A. Landing Feature Compatibility

The basic system architecture is depicted in Fig. 1. For the heterogeneous features possessed by each vehicle, we define a mapping from n_r vehicles to their corresponding feature bundle [24]

$$F \in \mathbb{R}^{n_r \times n_f},$$

where n_f denotes the length of each feature bundle, $F_{i,j}$ represents the specific value of the feature j owned by vehicle i.

Precisely, we consider features that could potentially result in landing failure, then the UAVs/USVs-to-feature bundle mappings denoted by $F^a \in \mathbb{R}^{n_a \times n_f}$ and $F^s \in \mathbb{R}^{n_s \times n_f}$ ($n_f = 2$) become

$$F^a = \begin{bmatrix} f^a_{1,1} & f^a_{1,2} \\ f^a_{2,1} & f^a_{2,2} \\ \vdots & \vdots \\ f^a_{n_a,1} & f^a_{n_a,2} \end{bmatrix}, \quad F^s = \begin{bmatrix} f^s_{1,1} & f^s_{1,2} \\ f^s_{2,1} & f^s_{2,2} \\ \vdots & \vdots \\ f^s_{n_s,1} & f^s_{n_s,2} \end{bmatrix},$$

where the first and second columns of F^a represent the diagonal length (m), i.e., the sum of the wheelbase and propeller diameter, and rated battery energy (Wh) of UAVs, respectively. The first and second columns of F^s represent the side length (m) of the square landing platform, and available charging energy (Wh) carried by USVs.

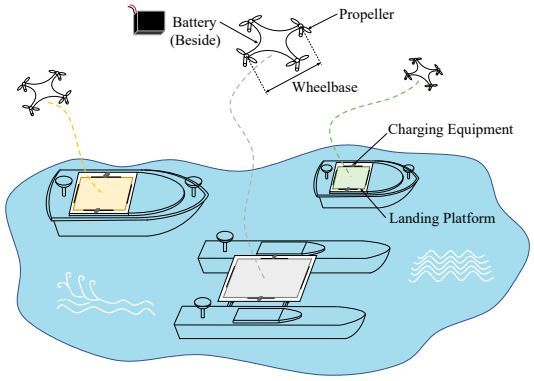

(a) Heterogeneous CDUUF illustration

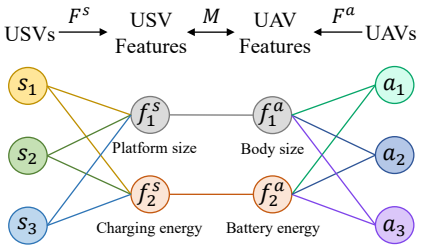

(b) Heterogeneous-feature matching mechanism

USVs	Features	
	f^s_1	f^s_2
s_1	0.4	85
s_2	0.6	180
s_3	1	200

UAVs	Features	
	f^a_1	f^a_2
a_1	0.3	70
a_2	0.55	100
a_3	0.85	175

(c) Notation

Fig. 2. (a) Illustration of the heterogeneous CDUUF consisting of 3 UAVs and 3 USVs (including two monohulls and a catamaran), vehicles in each species own distinct feature values. Each UAV selects the most suitable USV for landing, the consequent matching status and landing trajectories are shown in dash lines. (b) The matching mechanism of heterogeneous landing features possessed by UAVs and USVs. Only when all features between them are compatible, can the USV be considered as a viable candidate to accommodate the UAV. F^s and F^a denote the USVs/UAVs-to-feature bundle mappings, respectively. M is the resulting cooperative landing ability mapping. (c) The concrete feature values used in this example.

Furthermore, a cooperative landing ability between a USV and any UAV exists if and only if all feature requirements of the UAV are satisfied, i.e., the landing area on the USV should be larger than the UAV itself and the remaining charging energy should meet the needs of the UAV's battery. It can also be viewed as a *service-provider* and *service-receiver* connection.

To match vehicles in set $\mathcal{V}_1$ and $\mathcal{V}_2$ to accomplish the landing task, the cooperative landing ability mapping $M \in \{0,1\}^{n_s \times n_a}$ is defined as follows

$$M_{i,j} = \begin{cases} 1, & if\ F^s_{i,-} - F^a_{j,-} \geq 0 \\ 0, & \text{otherwise} \end{cases}, \tag{8}$$

where $M_{i,j} = 1$ if and only if USV i can supply all the demands of UAV j, $M_{i,-}$ represents the ith row of the matrix M, the inequality in (8) holds elementwise.

Assumption 1. *For the whole UAV group $\mathcal{V}_1$, there always exists at least one suitable USV that meets the specific*

landing feature requirements of UAV $j, j \in \mathcal{V}_1$, i.e.,

$$\sum_{i\in\mathcal{V}_2} M_{i,j} \geq 1, \quad \forall j \in \mathcal{V}_1.$$

Since the mapping M indicates whether a USV is a prospective candidate to be selected by a UAV, one has that the specialization matrix for UAV j is

$$M_j = \text{diag}(M_{-,j}) \in \mathbb{R}^{n_s\times n_s}, \tag{9}$$

where $M_{-,j}$ represents the jth column of the matrix M. An illustrative example of the heterogeneous CDUUF is given in Fig. 2, where the corresponding cooperative landing ability mapping M is calculated to be

$$M = \begin{bmatrix} 1 & 0 & 0 \\ 1 & 1 & 0 \\ 1 & 1 & 1 \end{bmatrix}.$$

B. Landing Convergence and Collision Avoidance

After calculating the cooperative landing ability mapping in Sec. III-A, we are ready to introduce two kinds of subtasks, namely, UAV-USV landing convergence and collision avoidance among UAVs in the landing mission.

Assumption 2. *Each USV in set $\mathcal{V}_2$ is able to accommodate at most one UAV.*

Firstly, the UAV-USV landing convergence is to ensure position and velocity convergence between the matched UAV and USV. However, the traditional CBF in [24] only remains on the single-integrator dynamic, which cannot be utilized for Eq. (5) because $L_g h(x,t) = 0$, i.e., $u(t)$ is not constrained [30].

To address this issue, we define the position error between the matched UAV i and USV j to be

$$e_{i,j}(t) = q_i(t) - \eta_j(t). \tag{10}$$

It follows from (5), (6) and (10) that

$$\dot{e}_{i,j}(t) = p_i(t) - \nu_j(t), \tag{11}$$

which implies that a candidate CLF $V_{i,j}(e_{i,j}, \dot{e}_{i,j})$ for UAV i and USV j to be

$$\begin{aligned} V_{i,j}(e_{i,j},\dot{e}_{i,j}) &= \frac{1}{2}\begin{bmatrix} e_{i,j}^\intercal & \dot{e}_{i,j}^\intercal \end{bmatrix} P \begin{bmatrix} e_{i,j}^\intercal & \dot{e}_{i,j}^\intercal \end{bmatrix}^\intercal \\ &= \frac{1}{2}\begin{bmatrix} e_{i,j}^\intercal & \dot{e}_{i,j}^\intercal \end{bmatrix} \begin{bmatrix} P_1 & P_2 \\ P_2^\intercal & P_3 \end{bmatrix} \begin{bmatrix} e_{i,j}^\intercal & \dot{e}_{i,j}^\intercal \end{bmatrix}^\intercal. \end{aligned} \tag{12}$$

Here, P denotes a symmetric, positive definite block matrix, i.e. P_1 and $P_3 - P_2^\intercal P_1^{-1} P_2$ are positive definite, P_2 is also positive definite. Using Definition 1, we can formulate the following constraint to ensure UAV-USV landing convergence

$$\dot{V}_{i,j}(e_{i,j},\dot{e}_{i,j}) + W_3(e_{i,j},\dot{e}_{i,j}) - \delta_{i,j} \leq 0, \tag{13}$$

where $W_3(e_{i,j}, \dot{e}_{i,j})$ is the positive definite function in Eq. (2), and $\delta_{i,j} \in \mathbb{R}^+$ is the corresponding slack variable. The validity of this constraint can be proved similarly to [31].

Secondly, it is imperative to uphold a safe distance between any pair of UAVs during the landing process. Analogous to [32], we first define the normal component $\bar{p}_{i,k}$ of the relative velocity between UAVs i and k to be

$$\bar{p}_{i,k} = \frac{q_{i,k}^\intercal}{\|q_{i,k}\|} p_{i,k}, \tag{14}$$

where $q_{i,k} := q_i - q_k, p_{i,k} := p_i - p_k$ are the relative position and velocity between UAVs i and k. Then, the candidate CBF $h_{i,k}$ is formulated to be

$$h_{i,k} = 2(\xi_i + \xi_k)(\|q_{i,k}\| - D_{\min}) - \bar{p}_{i,k}^2, \tag{15}$$

where ξ_i and ξ_k are the maximum braking accelerations of UAVs i and k, and $D_{\min}$ is the minimum allowed distance. Moreover, it follows from Definition 2 and Eq. (15) that the collision avoidance CBF constraint for UAVs becomes

$$\dot{h}_{i,k}(q_{i,k},p_{i,k}) + \varepsilon h_{i,k}^3(q_{i,k},p_{i,k}) \geq 0, \tag{16}$$

where $\gamma(h(x)) = \varepsilon h^3(x)$ with $\varepsilon > 0$.

C. Landing Algorithm

By incorporating the cooperative landing ability mapping M in Eq. (8) with the constraints of UAV-USV landing convergence in (13) and collision avoidance in (16) together, we can formulate the landing algorithm to be the following optimization problem, which is to generate an optimal assignment of the CDUUF and control the UAVs to approach the matched USVs at each point in time,

$$\min_{u,\delta,\alpha} \sum_{i=1}^{n_a} \left(C\|\Pi_i \alpha_{-,i}\|^2 + \|u_i\|^2 + l\|\delta_i\|_{M_i}^2\right) \tag{17a}$$

$$\text{s.t. } \dot{V}_{i,j}(e_{i,j},\dot{e}_{i,j}) + W_3(e_{i,j},\dot{e}_{i,j}) - \delta_{i,j} \leq 0 \tag{17b}$$

$$\dot{h}_{i,k}(q_{i,k},p_{i,k}) + \varepsilon h_{i,k}^3(q_{i,k},p_{i,k}) \geq 0 \tag{17c}$$

$$\delta_{i,m} \geq \kappa\left(\delta_{i,j} - \delta_{\max}(1-\alpha_{j,i})\right), \quad m \neq j \tag{17d}$$

$$\mathbf{1}_{n_s}^\intercal \alpha_{-,i} = 1 \tag{17e}$$

$$\mathbf{1}_{n_a}^\intercal \alpha_{j,-}^\intercal \leq 1 \tag{17f}$$

$$\|u_i\|_\infty \leq \xi_i \tag{17g}$$

$$\|\delta_i\|_\infty \leq \delta_{\max} \tag{17h}$$

$$\forall i,k \in \mathcal{V}_1, \forall j,m \in \mathcal{V}_2,$$

where $\alpha \in \{0,1\}^{n_s\times n_a}$, $C \in \mathbb{R}^+, l \in \mathbb{R}^+$ are scaling parameters used to reconcile between meeting the cooperative landing ability and minimizing the energy consumed by individual UAVs as much as possible. The cost function in (17a) is composed of three terms. In the first term, Π_i is a projection matrix that represents the orthogonal complement of the subspace spanned by M_i, which also indicates whether a USV is appropriate for UAV i to perform the landing task together. It is defined below

$$\Pi_i = I_{n_s} - M_i M_i^\dagger, \tag{18}$$

where I_{n_s} denotes the $n_s \times n_s$ identity matrix, $M_i^\dagger$ is the Moore-Penrose inverse of the specialization matrix M_i of UAV i. Let $M_i = \text{diag}([m_{i,1}, m_{i,2}, \ldots, m_{i,n_s}])$, if UAV i

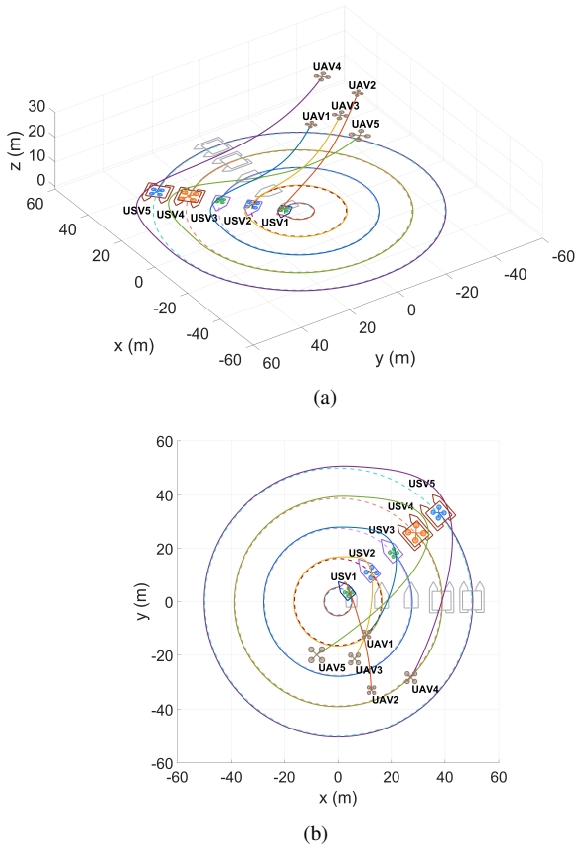

Fig. 3. (a) Coordinated landing trajectories of the CDUUF, where 5 UAVs $\{1, 2, 3, 4, 5\}$ from initial positions gradually perch on their corresponding matched USVs $\{3, 1, 2, 5, 4\}$. (b) In the top view, different types of UAVs and USVs are plotted in different sizes and colors. (Here, the quadcopter shapes represent the UAVs, and the monohull and catamaran shapes are the USVs. Their initial positions are illustrated in light brown and light gray, respectively.)

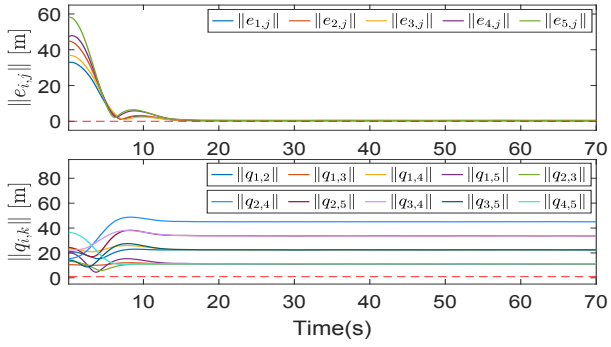

Fig. 4. Temporal evolution of the landing errors between the matched UAVs and USVs $\|e_{i,j}\|, i \in \mathcal{V}_1, j \in \mathcal{V}_2$, the inter-UAV distances $\|q_{i,k}\|, i, k \in \mathcal{V}_1, i \neq k$.

is unsuitable to land on USV t because of incompatible features, i.e. $m_{i,t} = 0$, then

$$\Pi_i = \text{diag}([\underbrace{0, \ldots, 0}_{t-1}, 1, \underbrace{0, \ldots, 0}_{n_s - t}]).$$

The second item $\|u_i\|^2$ represents the control effort spent by each UAV, which is proportional to energy consumption. The third item is the norm of δ_i weighted by the specialization matrix M_i, where $\|x\|^2_{M_i} = x^\intercal M_i x$, $x \in \mathbb{R}^{n_s}$, the slack variables between UAV i and its unsuitable USVs are not penalized. This ensures the position error and velocity error between the matched UAV and USV asymptotically settle to the equilibrium combined with (17b). The constraint (17c) guarantees collision avoidance between any two distinct UAVs in set $\mathcal{V}_1$ by keeping their distance above $D_{\min}$. Moreover, constraint (17d) implies that USV j has the highest priority for UAV i, where $\kappa > 1$ implies how the priorities influence the relative effectiveness of the UAV landing on different USVs, $\delta_{\max}$ is the maximum value of $|\delta_{i,j}|$. Constraints (17e) and (17f) ensure that each UAV has to land on only one USV and each USV can carry at most one UAV, respectively.

IV. Simulation

In this section, we validate the effectiveness of the proposed framework in two scenarios. The numerical simulations are performed in MATLAB using CVX [33] and Gurobi [34].

A. Coordinated Landing for USVs Moving along Closed Paths

First of all, we consider a CDUUF composed of 5 UAVs and 5 USVs, the USVs are maneuvering along prescribed concentric circular paths, with their respective feature values being provided as

$$F^a = \begin{bmatrix} 0.3 & 0.3 & 0.55 & 0.55 & 0.85 \\ 70 & 70 & 100 & 100 & 175 \end{bmatrix}^\intercal \quad (19)$$
$$F^s = \begin{bmatrix} 0.4 & 0.6 & 0.6 & 1 & 1 \\ 85 & 180 & 180 & 200 & 200 \end{bmatrix}^\intercal.$$

Specifically, the motion of the USVs can be described by

$$x_{j,1} = r_j \cos(\omega_1 t)\text{m}, \;\; x_{j,2} = r_j \sin(\omega_1 t)\text{m}, \;\; x_{j,3} = 0\text{m},$$

with the radii $r_1 = 5, r_2 = 16.25, r_3 = 27.5, r_4 = 38.75, r_5 = 50$, the constant angular velocity $\omega_1 = 0.1\,\text{rad/s}$. Initial positions of the UAVs are randomly generated with the heights between $25\,\text{m}$ and $30\,\text{m}$, and the initial distance between any pair of UAVs is set to be greater than $D_{\min} = 1\,\text{m}$. Moreover, the parameters of the optimization problem in (17) are chosen as $C = 10^5, l = 10^{-5}, \varepsilon = 0.5, \kappa = 10^5, \delta_{\max} = 10^4$ and $\xi_i = 10\,\text{m/s}^2, \forall i \in \mathcal{V}_1$.

As depicted in Fig. 3, 5 USVs are moving along five concentric circles, 5 UAVs $\{1, 2, 3, 4, 5\}$ are assigned to their respective optimal USVs $\{3, 1, 2, 5, 4\}$ and commence the landing procedure. The detailed information is also shown in Fig. 4 in terms of the landing errors and inter-UAV distances. It is observed that the landing errors asymptotically converge to be around zeros and the inter-UAV distances consistently maintain above the desired safe distance.

B. Coordinated Landing for USVs Moving along Open Paths

In this sequel, we carry out a simulation under more challenging conditions. We consider a CDUUF composed of 5 UAVs and 6 USVs, with the USVs following prescribed sinusoidal paths. Feature values of the UAV group remain

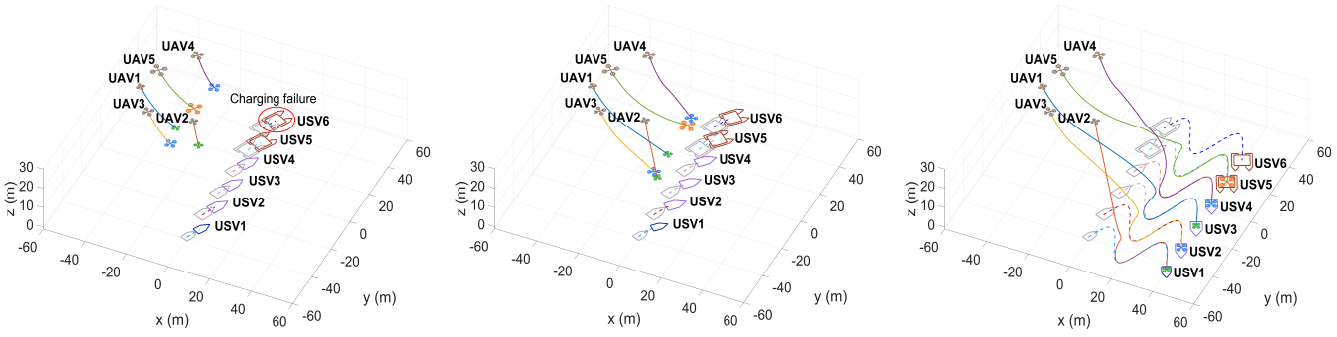

(a) t=3s (b) t=4.5s (c) t=40s

Fig. 5. Snapshots of coordinated landing trajectories of the CDUUF. (a) 5 UAVs $\{1, 2, 3, 4, 5\}$ are initially matched with USVs $\{4, 2, 3, 6, 5\}$ and progressively execute the landing maneuver. When $t = 3$s, the charging station carried by USV-6 breaks down (shown by the red ellipse), thus the corresponding feature value $f^s_{6,2}$ falls to zero. As a result, by solving the optimization problem (17), the UAVs are reassigned to USVs $\{3, 1, 2, 4, 5\}$ to continue landing. (b) UAV-4 and UAV-5 have the potential to collide due to the matching status variation. (c) 5 UAVs successfully landed on the matched USVs and no collision took place throughout the landing process. (Here, the quadcopter shapes represent the UAVs, and the monohull and catamaran shapes are the USVs. Their initial positions are illustrated in light brown and light gray, respectively.)

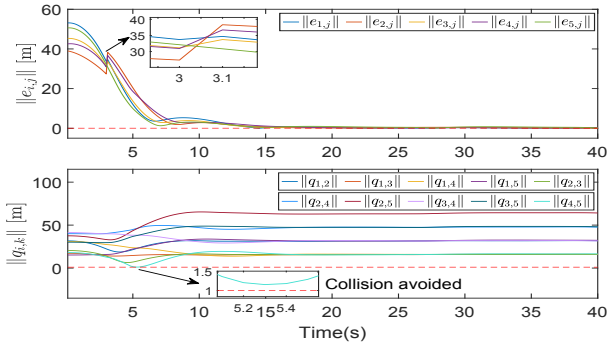

Fig. 6. Temporal evolution of the landing errors between the matched UAVs and USVs $\|e_{i,j}\|, i \in \mathcal{V}_1, j \in \mathcal{V}_2$, the inter-UAV distances $\|q_{i,k}\|, i, k \in \mathcal{V}_1, i \neq k$. The matching status changes at $t = 3$s and no collision occurred during the whole landing process.

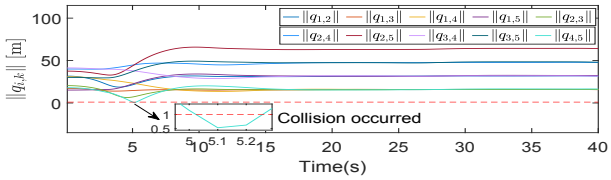

Fig. 7. Temporal evolution of the inter-UAV distances $\|q_{i,k}\|, i, k \in \mathcal{V}_1, i \neq k$ without collision avoidance constraints, UAV-4 and UAV-5 collide at $t = 5.1$s.

unchanged as (19), while the USVs-to-feature bundle mapping is modified to

$$F^s = \begin{bmatrix} 0.4 & 0.6 & 0.6 & 0.6 & 1 & 1 \\ 85 & 180 & 180 & 180 & 200 & 200 \end{bmatrix}^\intercal.$$

The sinusoidal paths for the USVs are set as

$$x_{j,1} = t\text{m},\ x_{j,2} = A\sin(\omega_2 t) + d_j\text{m},\ x_{j,3} = 0\text{m},$$

with the amplitude $A = 10$m, the constant angular velocity $\omega_2 = 0.25\,\text{rad/s}$, and the offsets $d_1 = -40, d_2 = -24, d_3 = -8, d_4 = 8, d_5 = 24, d_6 = 40$. To assess the resilience of the proposed algorithm against vehicle failures, USV-6 is intentionally designed to become incapable of charging after $t = 3$s. The optimization parameters for (17) are the same as the first case.

Snapshots of the simulation result are shown in Fig. 5. Fig. 5(a) depicts that 5 UAVs $\{1, 2, 3, 4, 5\}$ are initially moving toward USVs $\{4, 2, 3, 6, 5\}$. At $t = 3$s, USV-6 experiences a charging station failure, resulting in $M_{6,-} = 0$. Then 5 UAVs are reassigned to USVs $\{3, 1, 2, 4, 5\}$, which is also reflected in the landing error variations in Fig. 6. As seen in Fig. 5(b), UAV-4 and UAV-5 are approaching each other due to the change of matching status, thus trigger the safety constraint (17c). We can observe that all inter-UAV distances stay above $D_{\min}$ in Fig. 6. In contrast, when no collision avoidance constraint is imposed, UAV-4 and UAV-5 would collide at $t = 5.1$s as shown in Fig. 7. Finally, the UAVs settle to the matched USVs as exhibited in Fig. 5(c).

Remark 1. *In the above simulations, USVs are assumed to follow predefined paths with an emphasis on algorithm validation. However, it should be noted that the motion of USVs can be arbitrary. Additionally, our algorithm can exhibit resilience to weather influences, akin to its ability to withstand internal disturbance observed in Simulation 2, which will be discussed in our future work.*

V. Conclusion

In this paper, we have presented a multiple UAV-USV landing control algorithm for CDUUFs. The heterogeneous-feature matching strategy extracting landing-related features from UAVs and USVs has been proposed to construct a cooperative landing ability mapping. Then, a constraint-based optimization landing controller has been formulated, where suitable allocation requirements are incorporated, UAV-USV landing convergence and collision avoidance among UAVs are encoded into CLF and CBF constraints. The numerical simulations have demonstrated the effectiveness and resilience of the theoretical results. Future work will investigate real-world coordinated landing control for the CDUUF with environmental disturbances and communication delays.

REFERENCES

[1] B. Liu, H.-T. Zhang, H. Meng, D. Fu, and H. Su, "Scanning-chain formation control for multiple unmanned surface vessels to pass through water channels," *IEEE Transactions on Cybernetics*, vol. 52, no. 3, pp. 1850–1861, 2022.

[2] W. Meng, Z. He, R. Su, P. K. Yadav, R. Teo, and L. Xie, "Decentralized multi-UAV flight autonomy for moving convoys search and track," *IEEE Transactions on Control Systems Technology*, vol. 25, no. 4, pp. 1480–1487, 2017.

[3] B.-B. Hu, H.-T. Zhang, and Y. Shi, "Cooperative label-free moving target fencing for second-order multi-agent systems with rigid formation," *Automatica*, vol. 148, p. 110788, 2023.

[4] B.-B. Hu, Y. Zhou, H. Wei, Y. Wang, and C. Lv, "Ordering-flexible multi-robot coordination for moving target convoying using long-term task execution," *Automatica*, vol. 163, p. 111558, 2024.

[5] W. Yao, H. G. de Marina, B. Lin, and M. Cao, "Singularity-free guiding vector field for robot navigation," *IEEE Transactions on Robotics*, vol. 37, no. 4, pp. 1206–1221, 2021.

[6] B.-B. Hu, H.-T. Zhang, W. Yao, Z. Sun, and M. Cao, "Coordinated guiding vector field design for ordering-flexible multi-robot surface navigation," *IEEE Transactions on Automatic Control*, in press: 10.1109/TAC.2024.3355321, 2024.

[7] Y. Yan, Z. Chen, and V. Varadharajan, "Consensus of networked control multi-agent systems using a double-layer encryption scheme," *Journal of Automation and Intelligence*, vol. 2, no. 4, pp. 218–226, 2023.

[8] A. Hegde and D. Ghose, "Multi-UAV collaborative transportation of payloads with obstacle avoidance," *IEEE Control Systems Letters*, vol. 6, pp. 926–931, 2022.

[9] Z. Wang, X. Zhou, C. Xu, and F. Gao, "Geometrically constrained trajectory optimization for multicopters," *IEEE Transactions on Robotics*, vol. 38, no. 5, pp. 3259–3278, 2022.

[10] B.-B. Hu, H.-T. Zhang, B. Liu, H. Meng, and G. Chen, "Distributed surrounding control of multiple unmanned surface vessels with varying interconnection topologies," *IEEE Transactions on Control Systems Technology*, vol. 30, no. 1, pp. 400–407, 2021.

[11] B.-B. Hu, H.-T. Zhang, W. Yao, J. Ding, and M. Cao, "Spontaneous-ordering platoon control for multirobot path navigation using guiding vector fields," *IEEE Transactions on Robotics*, vol. 39, no. 4, pp. 2654–2668, 2023.

[12] B.-B. Hu, H.-T. Zhang, B. Liu, J. Ding, Y. Xu, C. Luo, and H. Cao, "Coordinated navigation control of cross-domain unmanned systems via guiding vector fields," *IEEE Transactions on Control Systems Technology*, vol. 32, no. 2, pp. 550–563, 2024.

[13] G. Shao, Y. Ma, R. Malekian, X. Yan, and Z. Li, "A novel cooperative platform design for coupled USV-UAV systems," *IEEE Transactions on Industrial Informatics*, vol. 15, no. 9, pp. 4913–4922, 2019.

[14] S. Lee, J. Lee, S. Lee, H. Choi, Y. Kim, S. Kim, and J. Suk, "Sliding mode guidance and control for UAV carrier landing," *IEEE Transactions on Aerospace and Electronic Systems*, vol. 55, no. 2, pp. 951–966, 2019.

[15] H.-T. Zhang, B.-B. Hu, Z. Xu, Z. Cai, B. Liu, X. Wang, T. Geng, S. Zhong, and J. Zhao, "Visual navigation and landing control of an unmanned aerial vehicle on a moving autonomous surface vehicle via adaptive learning," *IEEE Transactions on Neural Networks and Learning Systems*, vol. 32, no. 12, pp. 5345–5355, 2021.

[16] P. M. Gupta, É. Pairet, T. Nascimento, and M. Saska, "Landing a UAV in harsh winds and turbulent open waters," *IEEE Robotics and Automation Letters*, vol. 8, no. 2, pp. 744–751, 2023.

[17] R. Xu, C. Liu, Z. Cao, Y. Wang, and H. Qian, "A manipulator-assisted multiple UAV landing system for USV subject to disturbance," *arXiv preprint arXiv:2212.12196*, 2023.

[18] J. Ye, B.-B. Hu, Z. Xu, B. Liu, and H.-T. Zhang, "Autonomous landing allocation of multiple unmanned aerial vehicles on multiple unmanned surface vessels subject to energy consumption," in *International Conference on Intelligent Robotics and Applications*. Springer, 2021, pp. 611–621.

[19] N. Seenu, R. M. Kuppan Chetty, M. M. Ramya, and M. N. Janardhanan, "Review on state-of-the-art dynamic task allocation strategies for multiple-robot systems," *Industrial Robot*, vol. 47, no. 6, pp. 929–942, 2020.

[20] S. Park, Y. D. Zhong, and N. E. Leonard, "Multi-robot task allocation games in dynamically changing environments," in *2021 IEEE International Conference on Robotics and Automation (ICRA)*, 2021, pp. 8678–8684.

[21] X. Luo and M. M. Zavlanos, "Temporal logic task allocation in heterogeneous multirobot systems," *IEEE Transactions on Robotics*, vol. 38, no. 6, pp. 3602–3621, 2022.

[22] G. Notomista, S. Mayya, S. Hutchinson, and M. Egerstedt, "An optimal task allocation strategy for heterogeneous multi-robot systems," in *2019 18th European Control Conference (ECC)*, 2019, pp. 2071–2076.

[23] Y. Emam, S. Mayya, G. Notomista, A. Bohannon, and M. Egerstedt, "Adaptive task allocation for heterogeneous multi-robot teams with evolving and unknown robot capabilities," in *2020 IEEE International Conference on Robotics and Automation (ICRA)*, 2020, pp. 7719–7725.

[24] G. Notomista, S. Mayya, Y. Emam, C. Kroninger, A. Bohannon, S. Hutchinson, and M. Egerstedt, "A resilient and energy-aware task allocation framework for heterogeneous multirobot systems," *IEEE Transactions on Robotics*, vol. 38, no. 1, pp. 159–179, 2022.

[25] R. A. Freeman and P. V. Kototovic, *Robust Nonlinear Control Design: State-Space and Lyapunov Techniques*. USA: Birkhauser Boston Inc., 1996.

[26] A. D. Ames, S. Coogan, M. Egerstedt, G. Notomista, K. Sreenath, and P. Tabuada, "Control barrier functions: Theory and applications," in *2019 18th European Control Conference (ECC)*, 2019, pp. 3420–3431.

[27] X. Dong, B. Yu, Z. Shi, and Y. Zhong, "Time-varying formation control for unmanned aerial vehicles: Theories and applications," *IEEE Transactions on Control Systems Technology*, vol. 23, no. 1, pp. 340–348, 2015.

[28] B. Liu, Z. Chen, H.-T. Zhang, X. Wang, T. Geng, H. Su, and J. Zhao, "Collective dynamics and control for multiple unmanned surface vessels," *IEEE Transactions on Control Systems Technology*, vol. 28, no. 6, pp. 2540–2547, 2020.

[29] C. Tang, H.-T. Zhang, and J. Wang, "Flexible formation tracking control of multiple unmanned surface vessels for navigating through narrow channels with unknown curvatures," *IEEE Transactions on Industrial Electronics*, vol. 70, no. 3, pp. 2927–2938, 2022.

[30] W. Xiao and C. Belta, "High-order control barrier functions," *IEEE Transactions on Automatic Control*, vol. 67, no. 7, pp. 3655–3662, 2022.

[31] F. S. Barbosa, L. Lindemann, D. V. Dimarogonas, and J. Tumova, "Provably safe control of lagrangian systems in obstacle-scattered environments," in *2020 59th IEEE Conference on Decision and Control (CDC)*, 2020, pp. 2056–2061.

[32] L. Wang, A. D. Ames, and M. Egerstedt, "Safety barrier certificates for collisions-free multirobot systems," *IEEE Transactions on Robotics*, vol. 33, no. 3, pp. 661–674, 2017.

[33] M. Grant and S. Boyd, "CVX: Matlab software for disciplined convex programming, version 2.1," `http://cvxr.com/cvx`, Mar. 2014.

[34] Gurobi Optimization, LLC, "Gurobi optimizer reference manual," `https://www.gurobi.com`, 2023.